Overexpression of SPARC in Human Trabecular Meshwork Increases Intraocular Pressure and Alters Extracellular Matrix

Dong-Jin Oh,[1] Min Hyung Kang,[1] Yen Hoong Ooi,[2] Kyu Ryong Choi,[3] E. Helene Sage,[4] and Douglas J. Rhee[1]

[1]Department of Ophthalmology, Massachusetts Eye & Ear Infirmary, Harvard Medical School, Boston, Massachusetts
[2]Department of Pediatrics, New York Downtown Hospital, New York, New York
[3]Department of Ophthalmology, Ewha Womans University School of Medicine and Medical Center, Mokdong Hospital, Seoul, Korea
[4]Hope Heart Program, Benaroya Research Institute at Virginia Mason, Seattle, Washington

Correspondence: Douglas J. Rhee, Department of Ophthalmology, Massachusetts Eye & Ear Infirmary, 243 Charles Street, Boston, MA 02114; DougRhee@aol.com.

Submitted: November 23, 2012
Accepted: March 22, 2013

Citation: Oh D-J, Kang MH, Ooi YH, Choi KR, Sage EH, Rhee DJ. Overexpression of SPARC in human trabecular meshwork increases intraocular pressure and alters extracellular matrix. *Invest Ophthalmol Vis Sci*. 2013;54:3309–3319, DOI:10.1167/iovs.12-11362

Purpose. Intraocular pressure (IOP) regulation is largely unknown. SPARC-null mice demonstrate a lower IOP resulting from increased outflow. SPARC is a matricellular protein often associated with fibrosis. We hypothesized that SPARC overexpression would alter IOP by affecting extracellular matrix (ECM) synthesis and/or turnover in the trabecular meshwork (TM).

Methods. An adenoviral vector containing human SPARC was used to increase SPARC expression in human TM endothelial cells and perfused human anterior segments using multiplicities of infection (MOIs) 25 or 50. Total RNA from TM was used for quantitative PCR, while protein from cell lysates and conditioned media were used for immunoblot analyses and zymography. After completion of perfusion, the anterior segments were fixed, sectioned, and examined by light and confocal microscopy.

Results. SPARC overexpression increased the IOP of perfused human anterior segments. Fibronectin and collagens IV and I protein levels were elevated in both TM cell cultures and within the juxtacanalicular (JCT) region of perfused anterior segments. Collagen VI and laminin protein levels were increased in TM cell cultures but not in perfused anterior segments. The protein levels of pro-MMP-9 decreased while the kinetic inhibitors of metalloproteinases, TIMP-1 and PAI-1 protein levels, increased at MOI 25. At MOI 50, the protein levels of pro-MMP-1, -3, and -9 also decreased while PAI-1 and TIMP-1 and -3 increased. Only MMP-9 activity was decreased on zymography. mRNA levels of the collagens, fibronectin, and laminin were not affected by SPARC overexpression.

Conclusions. SPARC overexpression increases IOP in perfused cadaveric human anterior segments resulting from a qualitative change the JCT ECM. Selective decrease of MMP-9 activity is likely part of the mechanism. SPARC is a regulatory node for IOP.

Keywords: SPARC, adenovirus, matrix metalloproteinases, tissue inhibitors of matrix metalloproteinases, extracellular matrix, intraocular pressure, perfused anterior segment system

Primary open-angle glaucoma (POAG) is one of the leading causes of irreversible blindness.[1–3] Elevated intraocular pressure (IOP) is a causative risk factor for the development and progression of POAG.[4–6] The elevated IOP results from dysfunctional aqueous drainage through the trabecular meshwork (TM).[7,8] The exact molecular and cellular processes responsible for the normal physiologic regulation of outflow resistance in the TM remain elusive. However, shifting the equilibrium between extracellular matrix (ECM) synthesis and breakdown within the TM strongly influences IOP.[9–12] Furthermore, alterations of the ECM within the juxtacanalicular (JCT) portion of the TM have been found to be a primary pathophysiologic association with POAG.[13] Along with other investigators, we believe that proteins known to regulate ECM equilibrium in other tissues will influence IOP.[14]

Matricellular proteins are nonstructural, secreted glycoproteins that facilitate cellular control over their surrounding ECM and play a role in cellular adhesion in many human tissues.[15] The matricellular family includes SPARC (secreted protein, acidic and rich in cysteine), thrombospondins (TSPs) 1 and 2, tenascins C and X, hevin, and osteopontin.[15] Matricellular proteins, and in particular SPARC, are associated with increased fibrosis and aberrant tissue remodeling, processes implicated as major contributors to glaucoma pathogenesis.[15] In resting TM tissue and in TM cells undergoing physiologic stress (mechanical stretch), SPARC is one of the most highly transcribed genes, data indicating that SPARC has a prominent physiological function.[16–18] In response to transforming growth factor-β2, which is elevated in the aqueous humor of patients with POAG, SPARC is the most highly up-regulated protein.[19,20] Furthermore, we have demonstrated that SPARC-null mice have a 15%

to 20% lower IOP, the result of increased aqueous drainage.[21] These findings implicate SPARC as a significant regulator of IOP.

We hypothesized that SPARC regulates IOP by shifting the balance of ECM synthesis and turnover in the TM. Accordingly, we increased the expression of SPARC in cadaveric human perfused anterior segments and in cultured human TM cells by adenoviral transfection of cloned human SPARC. We measured the IOP, examined the drainage tissue via immunohistochemistry, and assessed the relative expression of various ECM components. In TM cells, the protein and mRNA levels of specific ECM proteins and matrix metalloproteinases (MMPs), which are prominent ECM-degrading enzymes in TM, and their kinetic inhibitors, tissue inhibitors of metalloproteinases (TIMPs), were determined.

Methods

Adenoviral Constructs and Adenovirus Production

Adenoviral (Av) vectors containing the human SPARC transgene (Av.hSPARC) and control Av vectors were produced by the use of the transpose-Ad adenoviral vector system (Qbiogene, Carlsbad, CA). A fragment of human SPARC cDNA (973 bp) was prepared by PCR of reverse-transcribed human mRNA, with human-specific primers, 5′ and 3′ ends containing *Nhe*1 and *Xba*1 restriction sites, which were subsequently cloned into the corresponding restriction site of pCR259 (Qbiogene). Transgene orientation was verified by analytical PCR. The pCR259 plasmid was prepared without SPARC as a control and both contain the CMV promoter and replication-deficient adenoviral genes (Av.Control). The Av plasmid, Av.CMV.hSPARC, was transformed in DH5α bacteria. The amplified DNA was purified (EndoFree Plasmid Maxi Kit; Qiagen, Valencia, CA) and was subsequently transfected into HEK293 packaging cells (QBI-293A) with the CalPhos Mammalian Transfection Kit (Clontech, Mountain View, CA). We incubated the packaging cells at 37°C, 5% CO_2 until the cytopathic effect become evident and collected the viral supernate. The Ad5.hSPARC adenovirus was purified and titered using the ViraBind adenovirus purification kit and QuickTiter adenovirus titer immunoassay kit (Cell Biolabs, San Diego, CA). The control Av plasmid, Av.CMV.empty, received the same handling except that the SPARC cDNA was not included in the plasmid.

Culture of Human TM Cells and SPARC Overexpression

Primary human TM cell cultures were derived from 12 separate donors (age range: 42–64 years; average age: 48.7 years). Maintenance growth medium consisted of Dulbecco's modified Eagle's medium (DMEM) supplemented with 20% fetal bovine serum (FBS; Invitrogen-Gibco, Grand Island, NY), 1% L-glutamine (2 mM), and 0.5% or 0.1% gentamicin (50 or 10 μg/mL). For each experiment, TM cultures were seeded into six-well plates (Costar, Corning, NY), allowed to grow to confluence at 37°C in a 10% CO_2 atmosphere and given an additional 2 to 3 days for differentiation. For all experiments, TM cells from the fourth or fifth passage were used.

TM cells were incubated in 2% FBS medium with Ad5.control or Ad5.hSPARC for 18 hours, after which 10% FBS medium and an equal volume were added to the 2% medium for an additional 24 hours (Fig. 1). TM cultures were incubated for another 24 hours in serum-free medium, which was later replaced with culture medium containing adenovirus for 24 hours. The serum-free conditioned medium was analyzed by immunoblot assays. Two different multiplicities of infection (MOIs; 25 and 50) of Ad5.control and Ad5.hSPARC were used. MOI is the ratio of infectious units to infectious targets (cells).[22,23] For zymographic analyses, gelatin (0.1%) for MMP-2 and -9 or β-casein (0.1%) for MMP-1 and -3 were mixed into liquid acrylamide during casting of the polyacrylamide gels. Concentrated conditioned medium mixed with 2× Tris-glycine-SDS zymography sample buffer at a 1:10 ratio was loaded onto 10% SDS-PAGE. The samples were subjected to electrophoresis at 130 V in tank buffer (250 mM Tris, 192 mM glycine, and 0.1% SDS). The gels were incubated with 2.5% Triton X-100 (renaturing buffer) with gentle agitation at room temperature, then transferred to enzyme assay buffer overnight at 37°C. The resultant gels were stained with 0.1% Coomassie Brilliant Blue G-250 (Bio-Rad, Hercules, CA) for at least 3 hours and were destained with fixing/destaining solution until clear bands were visible and contrasted well with the blue background. The gels were scanned using the Odyssey Infrared Imaging System (Li-Cor, Lincoln, NE), and relative densities of the bands were analyzed with the Odyssey densitometric software (version 1.2). All the MMPs were identified based on their molecular weights and were confirmed against purified MMP-1, -2, -3, and -9 (Chemicon, Temecula, CA) as positive controls.

Human Perfused Anterior Segment Culture System

All donor pairs of eyes (aged 42, 56, 78, 78, and 80 years) were obtained from National Disease Research Interchange (NDRI, Philadelphia, PA) according to the provisions of the Declaration of Helsinki for research involving human tissue. Eyes were obtained within 24 hours after death. No donors were known to have a history of glaucoma or other ocular disorder. Human perfused anterior segment cultures were prepared by scoring the surface of the eye around ora serrata with a surgical blade, and the full-thickness incision was completed around the eye with scissors. The vitreous, lens, and iris were removed. Ciliary processes were dissected carefully, leaving in place the longitudinal portion of the ciliary muscle. The anterior segments were rinsed thoroughly with culture media and were mounted into custom plexiglass culture chambers. Anterior segments were perfused at a constant flow rate of 2.5 μL/min with DMEM (Invitrogen-Gibco) containing 1% FBS, 1% L-glutamine (2 mM), penicillin (100 U/mL), streptomycin (100 U/mL), gentamicin (0.17 mg/mL), and amphotericin-B (0.25 μg/mL) under 5% CO_2 at 37°C, using microinfusion pumps (Harvard Apparatus, Holliston, MA). IOP was monitored with a pressure transducer (BD Medical, Franklin Lakes, NJ) and were recorded with an automated computerized system (National Instruments, Austin, TX) every second and averaged each hour. Perfused tissue was allowed to equilibrate at 37°C and 5% CO_2 until a stable baseline IOP was achieved, typically 2 to 4 days. Pairs of eyes were treated. The pairs were excluded if the eyes failed to achieve a stable baseline IOP ($n = 3$) or if the postexperimental toluidine blue–stained light microscopy sections showed acellularity ($n = 0$). Before injection, perfusion pumps were stopped briefly to lower the pressure in the anterior chamber of the eye. Then one eye was injected intracamerally with Ad5.control while the other received Ad5.hSPARC in a volume of 100 μL containing 1×10^8 infectious units (ifu), similar to the methodology described by Ethier et al.[24] The chambers were kept in a 5% CO_2, 37°C humidified incubator. The perfusate drained from scored episcleral veins. The perfusion chambers had a lid to protect against evaporation of media. Perfusate was collected using a sterile Pasteur pipette a day before and at 1 and 2 days after injection for immunoblot analysis of SPARC levels. After 5 days, the anterior segments were fixed and evaluated for viability and morphology by light microscopy at the termination of each study. Effects of SPARC overexpression on IOP were expressed as

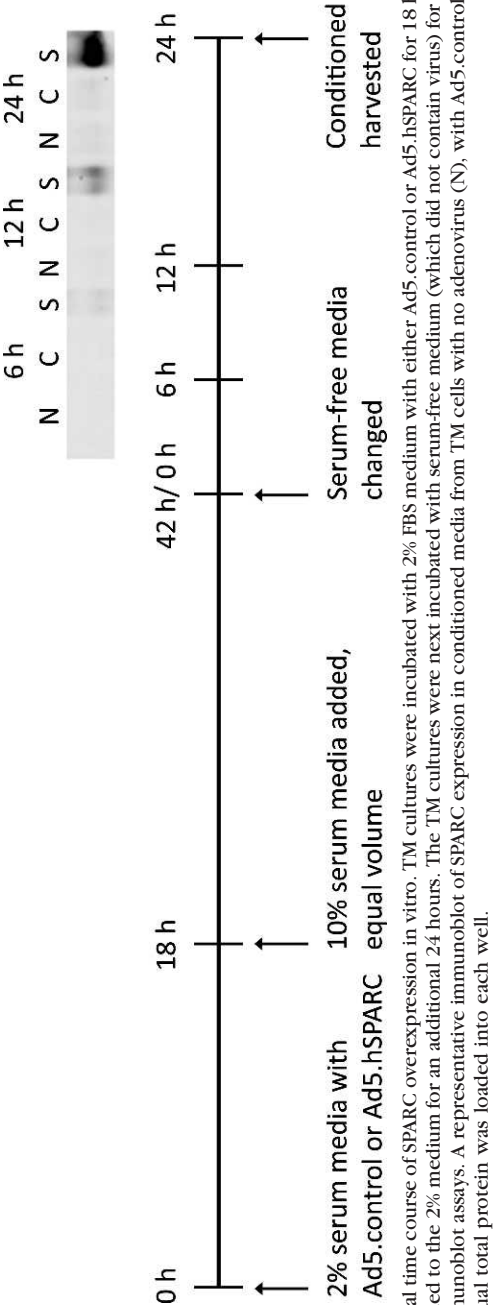

Figure 1. Experimental time course of SPARC overexpression in vitro. TM cultures were incubated with 2% FBS medium with either Ad5.control or Ad5.hSPARC for 18 hours. Then 10% FBS medium of equal volume were added to the 2% medium for an additional 24 hours. The TM cultures were next incubated with serum-free medium (which did not contain virus) for 24 hours. The serum-free media were harvested for immunoblot assays. A representative immunoblot of SPARC expression in conditioned media from TM cells with no adenovirus (N), with Ad5.control (C), and with Ad5.hSPARC (S+) infection is shown; equal total protein was loaded into each well.

the percentage change in IOP (compared to baseline values) over 96 hours. Values were expressed as mean ± SEM, and a paired two-tailed Student's *t*-test was applied to determine the significance of difference in IOP between control and experimental groups at selected time intervals. IOP was normalized at time point 0, the time of injection. Two-way ANOVA testing was applied to the mean IOP values after injection.

Quantitative PCR

Total RNA from TM endothelial cells was isolated using Trizol (Invitrogen, Carlsbad, CA) according to the manufacturer's protocol. Briefly, cultured TM cells were lysed with Trizol buffer, and chloroform was added. After centrifugation, total nucleic acid was isolated from the aqueous layer by ethanol precipitation. After digestion of DNA by DNase I, total RNA was isolated and stored at −80°C for no more than 1 month prior to further experiments.

Complementary DNA (cDNA) was synthesized using the M-MLV RT kit (Promega, Madison, WI) according to the manufacturer's instructions, with minor modifications. Briefly, 250 ng of total RNA was used as a template in 50 μL of reaction mixture containing 250 ng of oligo-dT primer, 1× reaction buffer, 0.2 mM of dATG, dCTG, dGTG, and dATG, 20 U of RNase inhibitor, and 200 U of M-MLV reverse transcriptase. The reaction mixture was incubated at 42°C for 1 hour and used for quantitative PCR (qPCR).

Quantitative PCR was performed to detect mRNA in cultured TM cells. Specific mRNAs were amplified in SYBR green I master mix (Applied Biosystems, Inc., Foster City, CA) with the ABI StepOnePlus (Applied Biosystems, Inc.). Quantification of the genes of interest was calculated by fold increase to β-actin expression using StepOne software v2.0 (Applied Biosystems, Inc.). All qPCR were performed in triplicate. Primers for human ECM types and β-actin were designed according to the Primer 3 program (http://frodo.wi.mit.edu) with an expected qPCR product of 200 bp (Table 1). Fold changes were normalized to GAPDH, then calculated relative to control (Ad5.control).

Immunoblot Analyses

Cultured TM cells infected with adenovirus were lysed in 1× radioimmunoprecipitation assay (RIPA) buffer (150 mM NaCl, 1% Igepal, 0.5% sodium deoxycholate, 0.1% SDS, 50 mM Tris-HCl, pH 8.0) with protease inhibitors (25 mTIU/mL aprotinin, 0.05 mg/mL phenylmethylsulfonyl fluoride, 1 mM EDTA, 1 mM EGTA, and 1 μg/mL leupeptin to a final volume of 1 mL with RIPA buffer). The conditioned media were collected and concentrated 30-fold with a centrifugal filter unit (Amicon Ultra-4, 10K; Millipore, Milford, MA). Equal amounts of total protein from conditioned media were mixed with 2× reducing buffer (125 mM Tris-HCl, pH 6.8, 4% SDS, 20% glycerol, 0.01% bromophenol blue) at a 1:10 ratio and were boiled for 3 minutes with reducing reagent (5 mg/mL dithiothreitol) or without it (nonreducing condition). The samples were analyzed by electrophoresis on 10% polyacrylamide gels (PAGE). SDS-PAGE was performed at 100 V in tank buffer with the XCell SureLock Mini-Cell system (Invitrogen). The separated proteins were transferred onto a nitrocellulose membrane with 0.45-μm pore size (Invitrogen) in blotting buffer (250 mM Tris-HCl, 192 mM glycine, and 10% methanol). The membrane was incubated for 1 hour in 0.5× blocking buffer (Rockland, Gilbertsville, PA) at room temperature. The membrane was next incubated with a primary antibody in 0.5× blocking buffer, overnight at 4°C (Table 2). The next day, the membrane was washed three times with TBS/T (50 mM Tris-HCl, 150 mM NaCl, 0.05% Tween20) for 10 minutes and incubated with IRDye™ 800-

Table 1. Primer Sequences for Quantitative PCR

	Forward	Reverse
Collagen α1 (I)	5′-CTGGTCCTGATGGCAAAACT-3′	5′-CTCCAGCCTCTCCATCTTTG-3′
Collagen α2 (IV)	5′-TCTTTCCTCATGCACACTGC-3′	5′-TTCAGCGTTTCAGACACAGG-3′
Collagen α1 (VI)	5′-CTGGGCGTCAAAGTCTTCTC-3′	5′-ATTCGAAGGAGCAGCACACT-3′
Collagen α2 (VI)	5′-GAGATCGACCAGGACACCAT-3′	5′-GGTCTCCCTGTCTTCCCTTC-3′
Collagen α3 (VI)	5′-CTGGGCAGACATACCATGTG-3′	5′-GCAAGTTCCTTCGTCTTTCG-3′
Fibronectin	5′-ACCAACCTACGGATGACTCG-3′	5′-GCTCATCATCTGGCCATTTT-3′
Laminin α5	5′-TGACCTTTTCTGGCTCGTCT-3′	5′-GTTCAGCACAAAGGGCTCTC-3′
Laminin β1	5′-AGGTTGGAGCTGCCTCAGTA-3′	5′-TGTTTTCACAACGCTTCTGC-3′
Laminin γ1	5′-GCATCTCTCGAGTGGTCCTC-3′	5′-TGGATAGGAATTGCCCTGAG-3′
β-actin	5′-GGCATCCTCACCCTGAAGTA-3′	5′-GGGGTGTTGAAGGTCTCAAA-3′

conjugated IgG (1:10,000; Rockland) for 1 hour (Table 2). The membrane was washed with 1× TBS/T three times at room temperature for 10 minutes and was scanned on the Odyssey Infrared Imaging System (Li-Cor). The band density of proteins was quantified with the Odyssey densitometric software (version 1.2). Deglycosylation of SPARC was performed using our previously described methodology.[18]

Immunofluorescent Staining

Paraffin-embedded TM tissue slides were deparaffinized in xylene for 15 minutes and incubated with xylene for a second 15-minute period. The slides were soaked with TBS/T for 5 minutes, hydrated with ethanol dilutions (100%, 95%, and 70%) for 5 minutes each, and rinsed with 1× TBS/T for 5 minutes. After excess liquid was removed, the tissues were made permeable with 0.2% Triton-100 in 1× PBS for 5 minutes, and were subsequently washed with TBS/T for 5 minutes. The tissues were incubated with blocking solution (10% normal goat serum in PBS) for 1 hour at room temperature and were washed with TBS/T for 10 minutes. Primary antibody (Table 1) diluted in blocking buffer was applied to each section at 4°C overnight. Optimal primary antibody concentrations were empirically determined by serial antibody dilution (1:50–1:200). Slides were washed three times with TBS/T for 10 minutes. Secondary antibodies (1:100) (Table 1) were applied to detect target protein, and nuclei were stained with TO-PRO-3 (1:200; Invitrogen). The slides were washed three times with TBS/T for 10 minutes, and a coverslip was applied with Immuno-Mount (Thermo Scientific, Pittsburgh, PA). Representative sections from two quadrants of each eye were analyzed. Labeled tissues were viewed under the Leica TCS SP2 spectral confocal laser scanning microscope (Leica Microsystems, Exton, PA). The secondary antibody-stained section was used to set up the parameters for nuclear (To-PRO-3) target ECM proteins (Alexa Fluor 488) and SPARC (Alexa Fluor 594) as the basal level. After these parameters were set and saved, we used these exact same conditions to analyze the expression of the target proteins in the remaining sections. Using the ImageJ software (National Institutes of Health, Bethesda, MD), we analyzed five areas selected randomly in the labeled tissues for the average pixel intensity in the green or red channels using arbitrary square box (width × height, 0.3 × 0.3).

Results

Effect of SPARC Overexpression on SPARC Levels in Human TM Cells

SPARC was expressed in the conditioned media by Ad5.hSPARC 14.43 ± 4.67 times at MOI 25 ($P = 0.015$) and 44.49 ± 14.52 times at MOI 50 ($P = 0.004$) in comparison to SPARC protein from the media of Ad5.control (Fig. 2A) treated cells. In the cell lysates, SPARC was increased 3.04 ± 1.35 times at MOI 25 ($P = 0.021$) and 9.45 ± 4.04 times at MOI 50 ($P = 0.001$; Fig. 2B). SPARC levels in the cell lysates were lower than that of the conditioned media. SPARC appeared only as a glycosylated band from the conditioned media, but as both an unglycosylated and a glycosylated band from the cell lysates (Fig. 2).

SPARC Overexpression in the Human Anterior Segment Culture System

After adenoviral infection of human anterior segments with Ad5.control or Ad5.hSPARC, we first confirmed that SPARC was in the perfusate. SPARC was increased 36.57 ± 2.29 times at 24 hours postinfection and 43.74 ± 4.06 times at 48 hours postinfection in Ad5.hSPARC-infected perfusate, compared to Ad5.control-infected perfusate ($n = 5$; Fig. 3A). SPARC levels were 13.45 ± 2.48 times higher ($n = 5$) in the TM tissue isolated from the anterior segments injected with Ad5.hSPARC, in comparison to the anterior segments injected with Ad5.control at the final day of the perfusion (Fig. 3B). Thus, Ad5.hSPARC increased SPARC expression within the TM tissue as well as secretion into the perfusate.

Effect of SPARC Overexpression on IOP in Human Anterior Segment Culture System. After intracameral injection of 1×10^8 ifu of adenoviruses, Ad5.control or Ad5.hSPARC, in paired constant-flow human anterior segment cultures ($n = 5$), the normalized IOP of Ad5.hSPARC increased an average of 24.31% ($P < 0.0001$) compared to Ad5.control. At baseline, the raw average IOPs for Ad5.control and Ad5.hSPARC were 10.06 ± 2.81 mm Hg and 12.59 ± 2.07 mm Hg (mean ± SEM), respectively, indicating that our scoring of the episcleral veins was appropriate. After 48 hours, the IOP

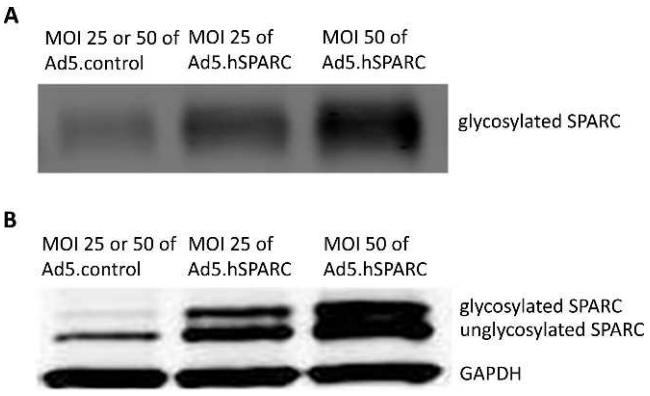

Figure 2. SPARC overexpression in vitro induced by Ad5.hSPARC. (**A**) Representative immunoblots from the conditioned media (**A**) and cell lysates (**B**) of cultured TM56 cells infected with Ad5.hSPARC. There was an increase of SPARC with increasing MOI ($n = 12$).

Table 2. Primary and Secondary Antibodies Used for Immunoblot and Immunofluorescence in This Study

Primary Antibody	Company	Antibody Host Species	Dilution	Secondary Antibody	Company	Dilution
Immunoblot						
MMPs						
MMP-1	R&D Systems	Mouse	1:1,000	IRDye 800 antimouse IgG	Rockland	1:10,000
MMP-2	R&D Systems	Mouse	1:1,000	IRDye 800 antimouse IgG	Rockland	1:10,000
MMP-3	R&D Systems	Mouse	1:1,000	IRDye 800 antimouse IgG	Rockland	1:10,000
MMP-9	R&D Systems	Mouse	1:500	IRDye 800 antimouse IgG	Rockland	1:10,000
ECM						
Collagen I	Rockland	Rabbit	1:10,000	IRDye 800 antirabbit IgG	Rockland	1:10,000
Collagen IV	Rockland	Rabbit	1:5,000	IRDye 800 antirabbit IgG	Rockland	1:10,000
Collagen VI	Rockland	Rabbit	1:5,000	IRDye 800 antirabbit IgG	Rockland	1:10,000
Fibronectin	Sigma-Aldrich	Rabbit	1:5,000	IRDye 800 antirabbit IgG	Rockland	1:10,000
Laminin	Sigma-Aldrich	Mouse	1:5,000	IRDye 800 antimouse IgG	Rockland	1:10,000
TIMPs						
TIMP-1	Chemicon	Rabbit	1:500	IRDye 800 antirabbit IgG	Rockland	1:10,000
TIMP-2	Chemicon	Rabbit	1:1,000	IRDye 800 antirabbit IgG	Rockland	1:10,000
TIMP-3	Chemicon	Rabbit	1:1,000	IRDye 800 antirabbit IgG	Rockland	1:10,000
TIMP-4	Chemicon	Rabbit	1:25,000	IRDye 800 antirabbit IgG	Rockland	1:10,000
Others						
PAI-1	Upstate	Rabbit	1:1,000	IRDye 800 antirabbit IgG	Rockland	1:10,000
SPARC	Haematologic Tech	Mouse	1:10,000	IRDye 800 antimouse IgG	Rockland	1:10,000
GAPDH	R&D Systems	Rabbit	1:2,500	IRDye 800 antirabbit IgG	Rockland	1:10,000
Immunofluorescence						
ECM						
Collagen I	Rockland	Rabbit	1:100	Goat antirabbit 488	Molecular Probes	1:200
Collagen IV	Rockland	Rabbit	1:100	Goat antirabbit 488	Molecular Probes	1:200
Collagen VI	Rockland	Rabbit	1:100	Goat antirabbit 488	Molecular Probes	1:200
Fibronectin	Sigma-Aldrich	Rabbit	1:100	Goat antirabbit 488	Molecular Probes	1:200
Laminin	Sigma-Aldrich	Mouse	1:100	Goat antirabbit 488	Molecular Probes	1:200
Others						
SPARC	Haematologic Tech	Mouse	1:500	Goat antimouse 594	Molecular Probes	1:200

of Ad5.hSPARC was significantly higher than Ad5.control ($P = 0.041$; Fig. 4A). The average increase of normalized IOPs between 48 and 98 hours was 27.93% ($P < 0.0001$) over the same time period. TM tissue infected by Ad5.control and Ad5.hSPARC adenovirus was stained with toluidine blue; there was no difference in cell viability of TM tissues (Fig. 4B).

Effect of SPARC Overexpression on ECM Proteins in Perfused Human Anterior Segments. After completion of perfusion, immunofluorescence of the anterior segments revealed that SPARC was increased 85 ± 51% by Ad5.hSPARC infection (Fig. 5, Table 3). In these segments, fibronectin as well as collagen types I and IV were increased compared to Ad5.control (Fig. 5, Table 3). Collagen type VI and laminin were not affected (Fig. 5, Table 3).

Effect of SPARC overexpression on ECM proteins, MMP, and TIMP levels in human TM cells

Effect of In Vitro SPARC Overexpression on ECM Protein Levels. Overexpression of SPARC was associated with increases in several ECM components (Table 4). Collagen IV was most affected and increased by 45.46 ± 15.83% at MOI 25 and 58.55 ± 15.67% at MOI 50 (Table 4, Fig. 6). Collagen types I and VI, fibronectin, and laminin were increased as well, but only at MOI 50 (Table 4, Fig. 6).

Effect of SPARC Overexpression In Vitro on MMP and TIMP Levels and Activity. At MOI 25, pro-MMP-9 was decreased. At MOI 50, pro-MMP-1, -3, and -9 were decreased (Table 4, Fig. 6). Pro-MMP-2 was not affected (Table 4, Fig. 6). Only TIMP-1 was significantly increased by 16.46 ± 4.71% at MOI 25. TIMP-1 and -3 increased at MOI 50 (Table 4, Fig. 5). TIMP-2 and -4 were unchanged (Table 4, Fig. 6). Expression of PAI-1, which also inhibits the activity of MMPs, was significantly increased by 23.28 ± 5.08% at MOI 25 and by 36.59 ± 7.92% at MOI 50 (Table 4, Fig. 6). Despite the changes in enzyme and inhibitor levels, zymography demonstrated that only MMP-9 activity was significantly decreased with the higher

Table 3. Fluorescence Intensity Measurements of ECM and SPARC Proteins From Immunofluorescent Images Postinjection of Ad5.control and Ad5.hSPARC (1×10^8 ifu)

ECM, $n = 5$	% Changes	*P* Value
Collagen I	54.54 ± 14.68	0.00027*
Collagen IV	59.29 ± 7.33	0.00005*
Collagen VI	37.07 ± 28.61	0.07210
Fibronectin	49.39 ± 24.72	0.00077*
Laminin	32.75 ± 22.97	0.09750
SPARC	84.85 ± 51.30	0.00059*

Measured by ImageJ software. The arbitrary fluorescence unit from the ImageJ software was used for the data.

* Indicates statistical significance.

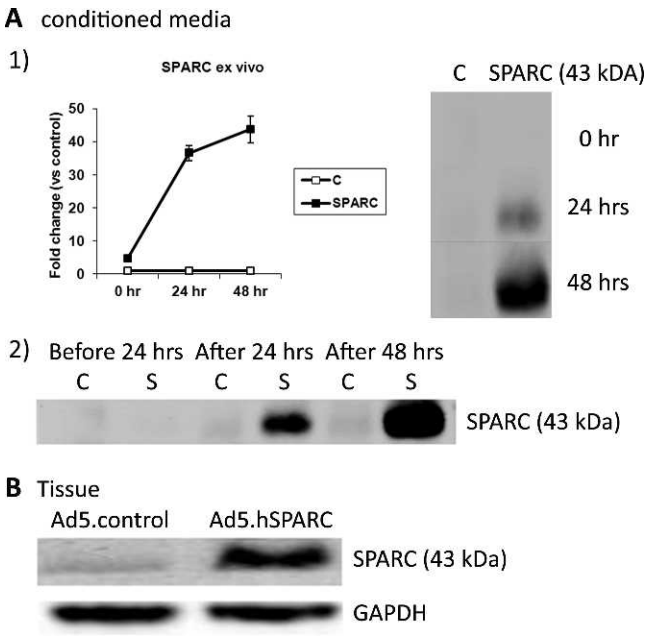

Figure 3. Immunoblot of SPARC from the perfused anterior segment culture system. SPARC levels were 36.57 ± 2.29 times greater ($n = 5$) at 24 hours postinfection and 43.74 ± 4.06 times ($n = 5$) greater at 48 hours postinfection in the perfused conditioned media compared with the perfusate sampled at time of adenovirus injection. C for ad5.control and SPARC for Ad5.hSPARC (**A1**). SPARC levels were shown in the perfused conditioned media 24 hours before, 24 hours after, and 48 hours after injection (**A2**). SPARC was 13.45 ± 2.48 times greater ($n = 5$) in the TM tissue isolated at the final day of the perfusion from the anterior segment injected with Ad5.hSPARC, compared with the anterior segment injected with Ad5.control (**B**). Representative immunoblots were taken from ex vivo Exp 4 TM78.

MOI; intermediate MMP-1 and active MMP-2 activity were unchanged (Table 4, Fig. 6).

Effect of SPARC Overexpression on the Relative Transcript Levels of Selected ECM Elements, MMPs, and TIMPs in Human TM Cells

The expression of various ECM mRNA transcripts was assessed by qPCR following Ad5.control or Ad5.hSPARC infection. Only collagen VI α3 expression was decreased by 58.34 ± 04.92% at MOI 25 ($P = 0.001$); however, there were no significant changes in any other ECM mRNAs (Table 5).

Discussion

In both perfused human anterior segments and cultured TM endothelial cells, we were able to increase SPARC expression in a dose-dependent manner. Methodologically, enhancing SPARC expression by viral transfection has the benefit of tissue/cell-specific posttranslational processing, which yields different results compared to those elicited by recombinant SPARC.[25] SPARC overexpression in the cell lysates was not as prominent as in the conditioned media, chiefly because SPARC is a secreted protein. In perfused human anterior segments, SPARC overexpression increased IOP without altering TM cell viability, as confirmed by toluidine blue stain. A high level of SPARC overexpression was required in order for the IOP to be significantly elevated. Due to the nature of using paired eyes from a single donor, only one control arm is possible. We

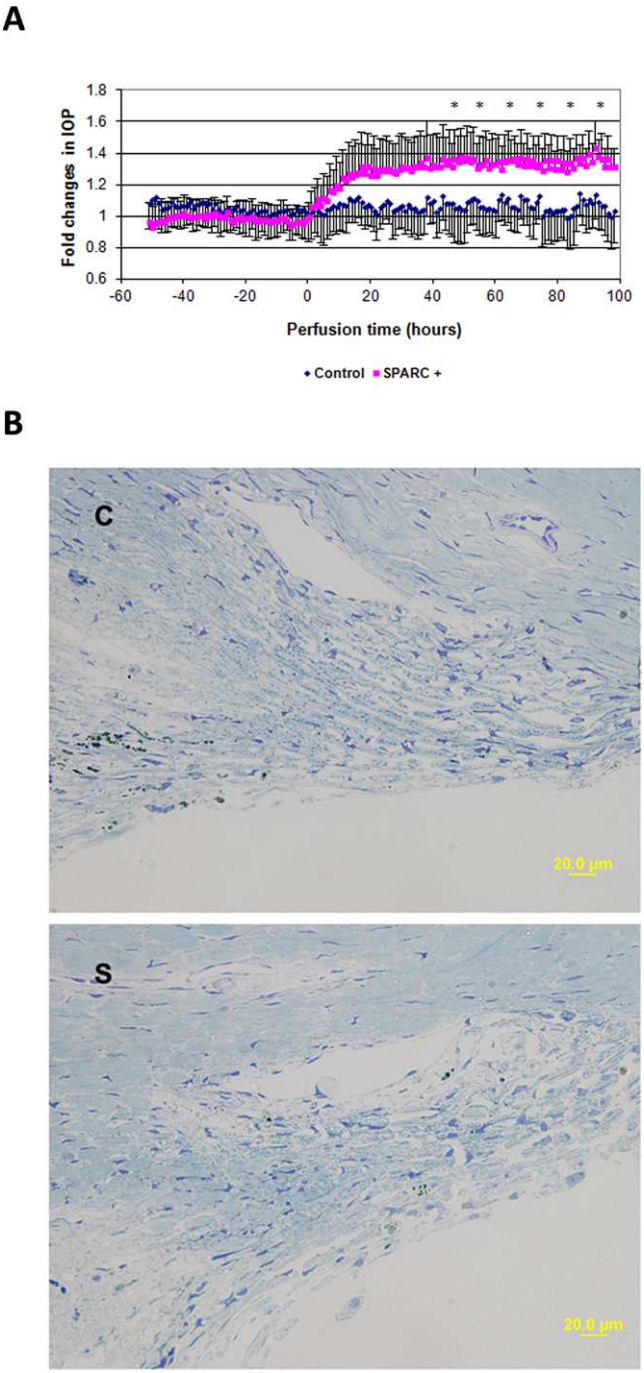

Figure 4. Effect of SPARC overexpression on IOP in the perfused anterior segments. (**A**) IOPs were measured in paired constant-flow human anterior segments ($n = 5$), injected intracamerally with 1×10^8 ifu of adenoviruses, Ad5.control (control), or Ad5.hSPARC (SPARC+). From 48 hours onward, the IOP for Ad5.hSPARC was significantly elevated compared to baseline control (*48, 55, 65, 75, 85, 95 hours; P values = 0.0410, 0.0419, 0.0236, 0.0090, 0.0196, 0.0014, respectively; $n = 5$). Paired t-tests were used for statistical significance. The IOPs were normalized to 1 at the zero hour time point. (**B**) TM tissue infected with 1×10^8 ifu of Ad5.control (C) and Ad5.hSPARC (S) adenovirus were stained with toluidine blue; there was no apparent difference in the cell viability of TM tissues infected ($n = 5$). ×200 magnification.

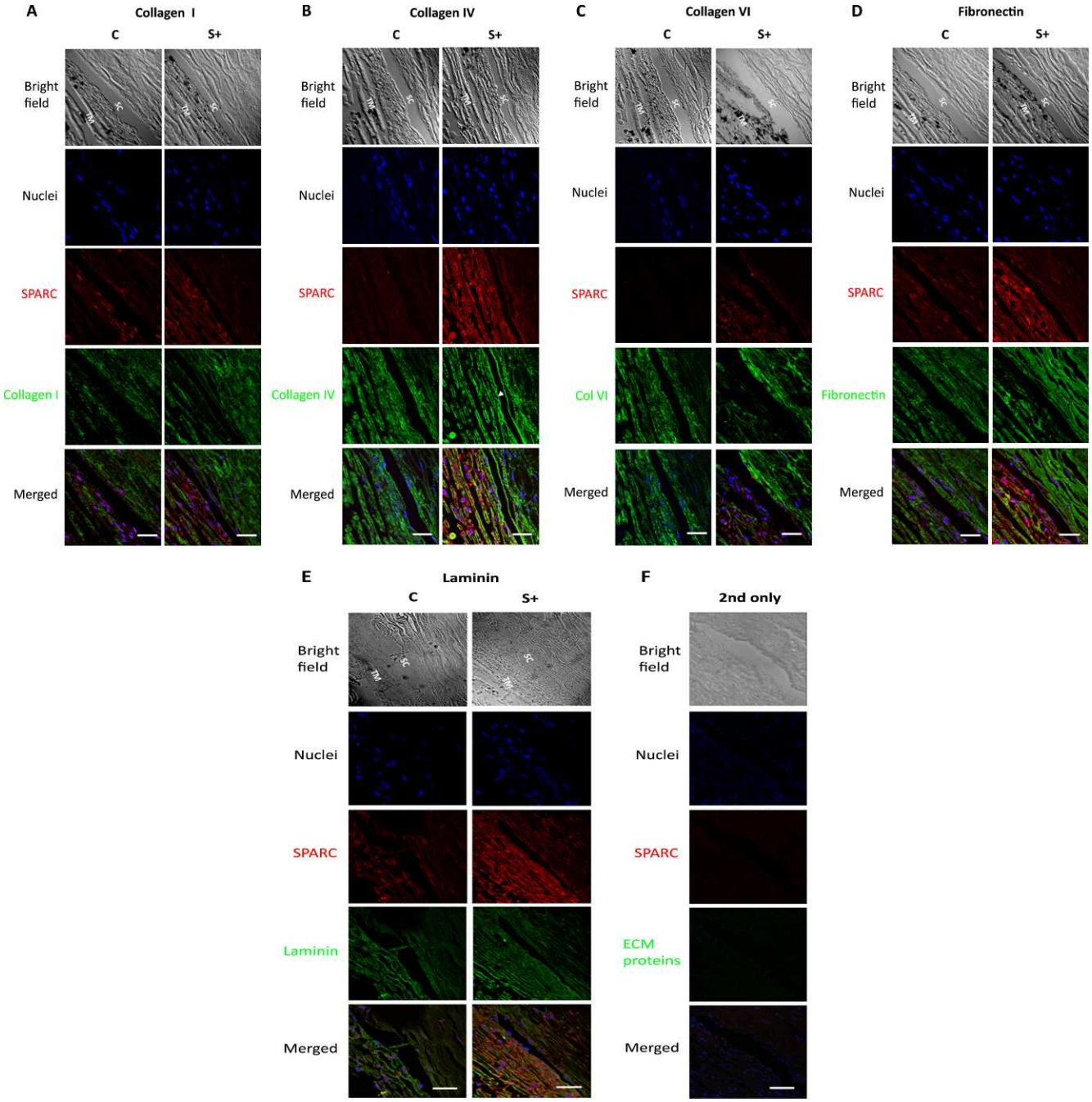

Figure 5. Representative immunolabeling of ECM proteins after infection with Ad5.control and Ad5.hSPARC (1×10^8 ifu). Collagen I (**A**), collagen IV (**B**), and fibronectin (FN) (**D**) were increased, but collagen VI (**C**) and laminin (LN) (**E**) were not changed. Collagen I was increased throughout the TM with some increase in the JCT region. Collagen IV was detected more prominently in the JCT region as well as under the outer wall of SC. Fibronectin was increased throughout the TM, but prominently within the JCT region. The secondary only staining (**F**) was shown as a negative control. *Scale bar*: 30 μm; C, control, S+, SPARC+; magnification = ×100.

selected the virus as the control as we were concerned about the virus itself being cytotoxic. Although we considered including a control protein to test if the elevated IOP is a nonspecific result of protein overload, it is unclear what similarly sized and completely inert protein would be appropriate. We believe that the finding of a qualitative difference in the JCT ECM, which was corroborated in TM cell culture, between experimental and control segments implicate that the elevation of IOP is the result of a functional effect of SPARC. Additionally, the overexpression of SPARC resulting in an elevation of IOP is consistent with our earlier report of a lower IOP in SPARC-null mice.[21]

The structure–function relationship, as demonstrated by immunohistologic examination of these segments, revealed an increase in fibronectin and collagen types IV and I within the JCT region; these ECM components were also elevated in TM endothelial cell cultures. Collagen type VI and laminin were increased in TM cell cultures at high levels of SPARC expression. The JCT region, consisting of Schlemm's canal (SC) inner wall cells, subendothelial ECM containing an

Table 4. Changes in the Protein Levels of Selected ECM Components, MMPs, TIMPs, and MMP Activity Following SPARC Overexpression in TM Cells

	% Change in Expression Compared to Control			
	MOI 25 (*n*)	*P* Value	MOI 50 (*n*)	*P* Value
MMPs (immunoblot)				
MMP-1	−8.69 ± 2.45 (7)	0.062	−18.26 ± 4.64 (7)	0.008*
MMP-2	0.27 ± 3.72 (8)	0.943	−16.46 ± 7.29 (8)	0.109
MMP-3	−5.45 ± 1.76 (6)	0.077	−23.87 ± 4.68 (6)	0.004*
MMP-9	−18.07 ± 4.33 (7)	0.042*	−25.26 ± 7.39 (7)	0.014*
MMPs (zymogram)				
MMP-1	1.64 ± 0.37 (8)	0.103	2.46 ± 0.89 (8)	0.078
MMP-2	−2.12 ± 3.24 (12)	0.527	−7.19 ± 5.85 (12)	0.245
MMP-9	−10.24 ± 3.56 (8)	0.023*	−18.32 ± 4.20 (8)	0.003*
ECM				
Collagen I	5.19 ± 1.84 (5)	0.098	19.18 ± 2.99 (5)	0.037*
Collagen IV	45.46 ± 15.83 (7)	0.028*	58.55 ± 15.67 (7)	0.010*
Collagen VI	5.54 ± 1.98 (7)	0.092	22.49 ± 5.43 (7)	0.002*
Fibronectin	9.87 ± 2.52 (6)	0.061	25.93 ± 9.65 (6)	0.002*
Laminin	7.12 ± 2.67 (5)	0.106	17.27 ± 3.25 (5)	0.006*
TIMPs				
TIMP-1	16.46 ± 4.71 (7)	0.013*	18.87 ± 6.95 (7)	0.038*
TIMP-2	10.11 ± 2.91 (6)	0.065	14.66 ± 3.27 (6)	0.300
TIMP-3	2.83 ± 1.54 (8)	0.158	17.75 ± 6.88 (8)	0.036*
TIMP-4	9.09 ± 5.31 (7)	0.062	8.61 ± 9.30 (7)	0.082
Other				
PAI-1	23.28 ± 5.08 (8)	0.003*	36.59 ± 7.92 (8)	0.002*

The data are shown as mean ± SEM.

incomplete basement membrane, and TM endothelial cells represent the anatomic location of maximal outflow resistance.[26–29] The regulation of IOP in the JCT region is a complex system with overlapping redundancy to compensate for the numerous physiologic stressors and perturbations. A few processes that have been shown to influence IOP include the regulation of ECM homeostasis,[9–12,14,30,31] the actin cytoskeleton and cellular tone of JCT TM and inner wall SC cells,[32] and the number of transcellular pores through inner wall SC cells.[33]

In both corneoscleral and JCT TM, the basement membrane is primarily comprised of collagen IV, fibronectin, and laminin.[34–36] An increase of basement membrane components, collagen IV, and fibronectin within the JCT TM is a significant structural finding in corticosteroid-induced glaucoma, in which there is an elevation of IOP from increased TM resistance.[37–40] In monolayers of TM endothelial cells, high glucose and dexamethasone each induced collagen type IV and laminin, changes resulting in decreased permeability.[41] In ex vivo porcine eyes, overexpression of a constitutively active mutant form of RhoA GTPase increased IOP through greater contractility of inner wall SC cells and increased JCT collagen type IV, fibronectin, and laminin.[42] The increase of JCT basement membrane material seen in our experiments correlates with compromised TM drainage and is likely a significant contributor to the mechanism of increased IOP caused by SPARC overexpression.

Table 5. Changes in the mRNA Levels of Selected ECM Proteins Compared With Controls as a Result of Adenoviral Infection by Ad5.control and Ad5.hSPARC

	% Change in Expression Compared to Control	
	MOI 25, $n = 6$	MOI 50, $n = 6$
Collagen I α1	−17.17 ± 11.28	−21.60 ± 15.13
Collagen IV α6	−7.81 ± 9.50	8.56 ± 27.17
Collagen VI α1	−17.92 ± 13.73	−7.24 ± 15.03
Collagen VI α2	−10.37 ± 14.05	23.55 ± 30.01
Collagen VI α3	−58.34 ± 4.92	32.69 ± 78.35
Fibronectin	7.18 ± 10.18	43.53 ± 45.12
Laminin α5	−32.20 ± 10.77	−27.11 ± 11.30
Laminin β1	−12.55 ± 14.69	9.79 ± 21.17
Laminin γ1	−30.51 ± 25.05	17.00 ± 40.82

The data are shown as mean ± SEM.
* $P < 0.05$).

We observed an increase of collagen type I within the JCT region after overexpression of SPARC. However, in TM cells, collagen type I was only increased by the greater degree of SPARC overexpression (MOI 50). Collagen types IV and VI are the predominant collagens in TM,[36,43] but collagen type I is an important structural element.[43] Transgenic mice with a mutation in the α1 subunit of type I collagen that prevents turnover have an elevated IOP due to the increased accumulation within the TM and sclera.[44]

Although collagen VI and laminin were not statistically elevated in the sections of perfused anterior segments, they were increased and almost reached significance. It is possible that with a large sample size, the 33% to 37% increases could reach statistical significance. Thus, these proteins could be part of the qualitative difference in ECM that increased IOP but were altered at a level below the statistical power of our study to definitively discern. In TM cell culture, the mRNA level of collagen VIα3 (Col6A3) was decreased while the protein level of collagen VI was unchanged. Col6A3 is one of the three α chains of type VI collagen and is larger than the α1 and α2 chains due to an increase in the number of subdomains found

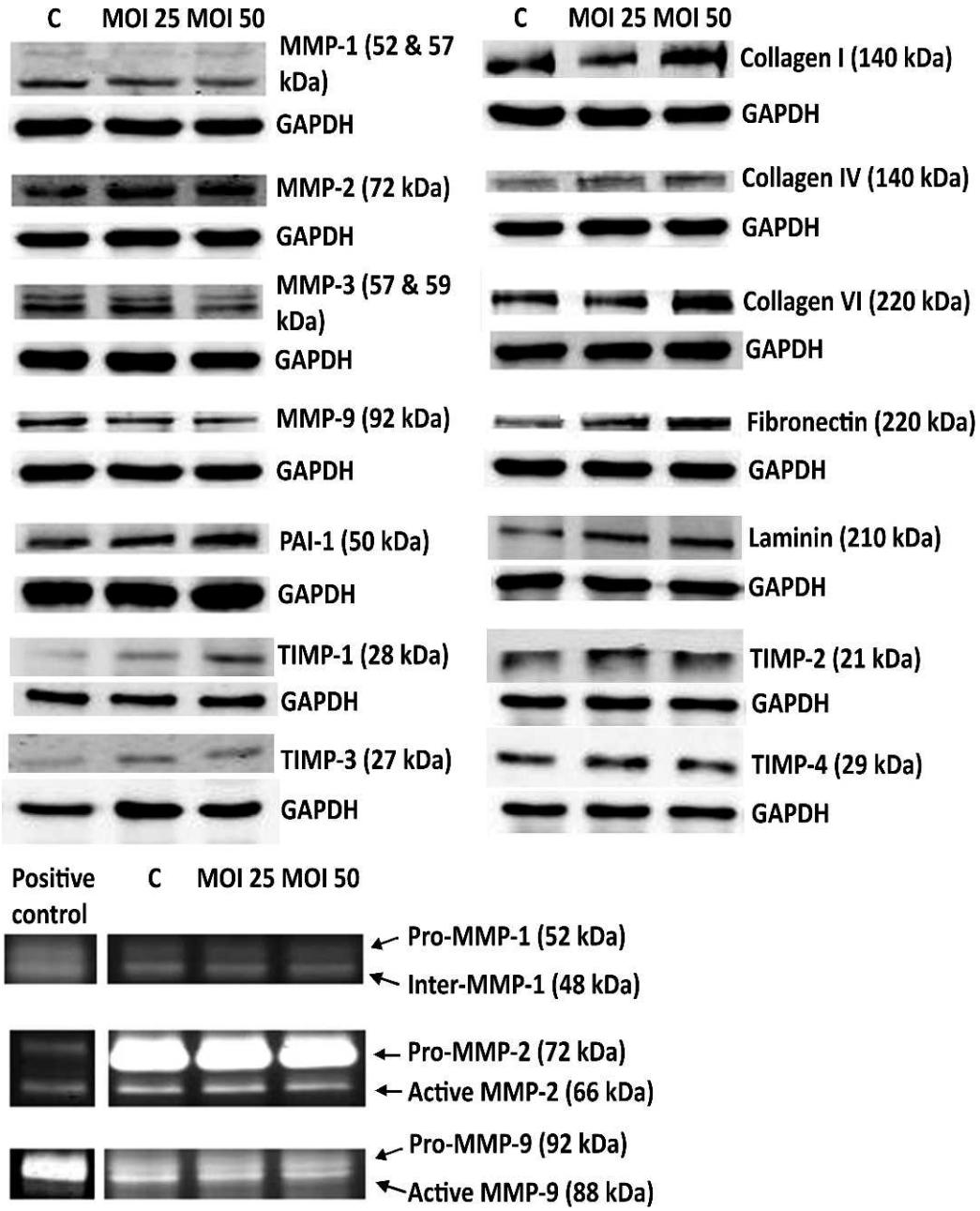

FIGURE 6. Representative immunoblots demonstrating relative changes in the levels of selected ECM proteins, MMPs, and TIMPs induced by SPARC overexpression in TM cells. At MOI 25, pro-MMP-9 was decreased, while the inhibitors TIMP-1 and PAI-1 as well as collagen IV were increased. At the higher MOI 50, pro-MMP-1, -3, and -9 were decreased while the inhibitors TIMP-1 and -3; PAI-1; collagen I, IV, and VI; fibronectin; and laminin were increased. At both MOIs 25 and 50, only the activity of MMP-9 was decreased.

in the amino terminal globular domain.[45,46] These domains have been shown to bind ECM proteins that assist with organizing matrix components.[47–49] The exact significance of the decrease of Col6A1 is unknown, but it may be a negative feedback loop designed to keep the level of collagen VI unchanged while SPARC is acting by a mechanism, other than a simple increase of translation, which could potentially enhance the level of collagen VI if unchecked.

The mechanistic pathways by which SPARC mediates these changes are unclear. The mRNA levels of these ECM proteins were not elevated results indicating that the mechanism is not a simple increase in production. SPARC may act as a chaperone, a posttranslational control, to stabilize ECM proteins or mRNA allowing for selective accumulation.[50–52] In both TM and uveoscleral pathways, alterations of MMP/TIMP balance correlate with aqueous drainage and IOP.[11,53,54] Despite the dose–response related shift in MMP/inhibitor balance of several MMPs, only MMP-9 activity was decreased on zymography. The selective decrease of MMP enzymatic activity is indicative of a qualitative change in composition of the JCT ECM rather than a simple, quantitative increase of ECM components. This assertion is consistent with our observation in SPARC-null mice, which have a lower IOP and enhanced aqueous drainage, but no observable quantitative changes in the JCT ECM at the light microscopy level.[21] Because the ECM of the JCT region is undergoing constant turnover, we hypothesized that the decrease of MMP-9 activity allows for the selective accumulation via decreased turnover of these

ECM products. We only studied MMPs-1, -2, -3, and -9. Previously we showed that TM cells also express MMPs-11, -12, -14, -15, -16, -17, -19, and -24, and it is possible that some of the other MMPs could also be affected by SPARC.[54]

Additionally, we believe that SPARC assists the posttranslational processing of collagen. The absence of SPARC is associated with a decreased capacity to compose organized mature collagen fibers.[55] SPARC plays a critical role in collagen fibril formation, recognizing the GVMGFO motif of the collagen triple helix.[56] In TIMP-2 null mice, there was a greater level of fibrosis that was due to increased SPARC and posttranslational stabilization of collagen fibers rather than increased collagen synthesis.[57]

The effects of SPARC modulation on various ECM proteins seen in our study are consistent with previous studies. In pulmonary fibroblasts, SPARC overexpression increased PAI via activation of Akt.[58] In tumor cells, SPARC overexpression resulted in a decrease in pro-MMP-9.[59] Other groups have examined the effects of SPARC suppression. Tumors grown in SPARC-null mice exhibited reduced deposition of fibrillar collagen types I and III, basement membrane collagen IV, and the collagen-associated proteoglycan decorin.[60] SPARC suppression in liver cells resulted in a decrease in collagen type I.[61] Using targeted siRNA to SPARC, Wei et al.[62] found that fibronectin was decreased. These observations with SPARC suppression are supportive of our findings with overexpression of SPARC.

ECM deposition and turnover are likely regulated by several mechanistic pathways. We have shown that SPARC regulates IOP through a coordinated response involving increased levels of certain ECM proteins in conjunction with a selective decrease of enzymatic activity, resulting in qualitative changes in the JCT ECM. The results within this report, along with our previous observation that SPARC-null mice have a lower IOP and enhanced aqueous outflow, strongly implicate a regulatory role for SPARC in IOP. Work is ongoing to determine the up- and down-stream signaling pathways for SPARC in TM as well as the mechanism responsible for these qualitative changes in the JCT ECM.

Acknowledgments

Disclosure: **D.-J. Oh**, None; **M.H. Kang**, None; **Y.H. Ooi**, None; **K.R. Choi**, None; **E.H. Sage**, None; **D.J. Rhee**, None

Supported by National Eye Institute Grants EY 019654-01 and EY 014104 (MEEI Vision-Core Grant), Research to Prevent Blindness, Massachusetts Lions Eye Research Foundation, and American Glaucoma Society.

References

1. Weinreb RN. Glaucoma neuroprotection: what is it? Why is it needed? *Can J Ophthalmol*. 2007;42:396–398.
2. Quigley HA. Number of people with glaucoma worldwide. *Br J Ophthalmol*. 1996;80:389–393.
3. Friedman DS, Wolfs RC, O'Colmain BJ, et al.; and the Eye Diseases Prevalence Research Group. Prevalence of open-angle glaucoma among adults in the United States. *Arch Ophthalmol*. 2004;122:532–538.
4. Kass MA, Heuer DK, Higginbotham EJ, et al.; and the Ocular Hypertension Treatment Study Group. The Ocular Hypertension Treatment Study: a randomized trial determines that topical ocular hypotensive medication delays or prevents the onset of primary open-angle glaucoma. *Arch Ophthalmol*. 2002;120:701–713.
5. Heijl A, Leske MC, Bengtsson B, Hyman L, Bengtsson B, Hussein M; for the Early Manifest Glaucoma Trial Group. Reduction of intraocular pressure and glaucoma progression. *Arch Ophthalmol*. 2002;120:1268–1279.
6. Collaborative Normal-Tension Glaucoma Study Group. Comparison of glaucomatous progression between untreated patients with normal-tension glaucoma and patients with therapeutically reduced intraocular pressures. *Am J Ophthalmol*. 1998;126:487–497.
7. Larsson LI, Rettig ES, Brubaker RF. Aqueous flow in open-angle glaucoma. *Arch Ophthalmol*. 1995;113:283–286.
8. Brubaker RF. Clinical measurements of aqueous dynamics: implications for addressing glaucoma. In: Civan MM, ed. *The Eye's Aqueous Humor: From Secretion to Glaucoma*. Vol. 45. San Diego: Academic Press; 1998:233–284.
9. Knepper PA, Farbman AI, Telser AG. Exogenous hyaluronidases and degradation of hyaluronic acid in the rabbit eye. *Invest Ophthalmol Vis Sci*. 1984;25:286–293.
10. Barany EH, Scotchbrook S. Influence of testicular hyaluronidase on the resistance to flow through the angle of the anterior chamber. *Acta Physiol Scand*. 1954;30:240–272.
11. Bradley JMB, Vranka J, Colvis CM, et al. Effect of matrix metalloproteinases activity on outflow in perfused human organ culture. *Invest Ophthalmol Vis Sci*. 1996;39:2649–2658.
12. Keller KE, Bradley JM, Kelley MJ, Acott TS. Effects of modifiers of glycosaminoglycan biosynthesis on outflow facility in perfusion culture. *Invest Ophthalmol Vis Sci*. 2008;49:2495–2505.
13. Rohen JW, Lutjen-Drecoll E, Flugel C, Meyer M, Grierson I. Ultrastructure of the trabecular meshwork in untreated cases of primary open-angle glaucoma (POAG). *Exp Eye Res*. 1993;56:683–692.
14. Keller KE, Aga M, Bradley JM, Kelley MJ, Acott TS. Extracellular matrix turnover and outflow resistance. *Exp Eye Res*. 2009;88:672–682.
15. Rhee DJ, Haddadin RI, Kang MH, Oh DJ. Matricellular proteins in the trabecular meshwork. *Exp Eye Res*. 2009;88:694–703.
16. Vittal V, Rose A, Gregory KE, Kelley MJ, Acott TS. Changes in gene expression by trabecular meshwork cells in response to mechanical stretching. *Invest Ophthalmol Vis Sci*. 2005;46:2857–2868.
17. Tomarev SI, Wistow G, Raymond V, Dubois S, Malyukova I. Gene expression profile of the human trabecular meshwork: NEIBank sequence tag analysis. *Invest Ophthalmol Vis Sci*. 2003;44:2588–2596.
18. Rhee DJ, Fariss RN, Brekken R, Sage EH, Russell P. The matricellular protein SPARC is expressed in human trabecular meshwork. *Exp Eye Res*. 2003;77:601–607.
19. Bollinger KE, Crabb JS, Yuan X, Putliwala T, Clark AF, Crabb JW. Quantitative Proteomics: TGFb2 signaling in trabecular meshwork cells. *Invest Ophthalmol Vis Sci*. 2011;52:8287–8294.
20. Tripathi R, Li J, Chan W, Tripathi B. Aqueous humor in glaucomatous eyes contains an increased level of TGF-beta 2. *Exp Eye Res*. 1994;59:723–727.
21. Haddadin RI, Oh DJ, Filipoppopolous T, et al. SPARC-null mice exhibit lower intraocular pressures. *Invest Ophthalmol Vis Sci*. 2009;50:3771–3777.
22. Mocanu JD, Yip KW, Alajez NM, et al. Imaging the modulation of adenoviral kinetics and biodistribution for cancer gene therapy. *Mol Ther*. 2007;15:921–929.
23. Mesonero A, Suarez DL, van Santen E, Tang DC, Toro H. Avian influenza in ovo vaccination with replication defective recombinant adenovirus in chickens: vaccine potency, antibody persistence, and maternal antibody transfer. *Avian Dis*. 2011;55:285–292.
24. Ethier CR, Wada S, Chan D, Stamer WD. Experimental and numerical studies of adenovirus delivery to outflow tissues of perfused human anterior segments. *Invest Ophthalmol Vis Sci*. 2004;45:1863–1870.

25. Atorrasagasti C, Malvicini M, Aquino JB, et al. Overexpression of SPARC obliterates the in vivo tumorigenicity of human hepatocellular carcinoma cells. *Int J Cancer*. 2010;126:2726–2740.
26. Moses RA, Grodzki WJ, Etheridge EL, Wilson CD. Schlemm's canal: the effect of intraocular pressure. *Invest Ophthalmol Vis Sci*. 1981;20:61–68.
27. Maepea O, Bill A. Pressures in the juxtacanalicular tissue and Schlemm's canal in monkeys. *Exp Eye Res*. 1992;54:879–883.
28. Maepea O, Bill A. The pressures in the episcleral veins, Schlemm's canal and trabecular meshwork in monkeys: effects of changes in intraocular pressure. *Exp Eye Res*. 1989;49:645–663.
29. Seiler T, Wollensak J. The resistance of the trabecular meshwork to aqueous humor outflow. *Graefes Arch Clin Exp Ophthalmol*. 1985;223:88–91.
30. Fuchshofer R, Tamm ER. Modulation of extracellular matrix turnover in the trabecular meshwork. *Exp Eye Res*. 2009;88:683–388.
31. Liton PB, Gonzalez P, Epstein DL. The role of proteolytic cellular systems in trabecular meshwork homeostasis. *Exp Eye Res*. 2009;88:724–728.
32. Tian B, Gabelt BT, Geiger B, Kaufman PL. The role of the actomyosin system in regulating trabecular fluid outflow. *Exp Eye Res*. 2009;88:713–717.
33. Overby DR, Stamer WD, Johnson M. The changing paradigm of outflow resistance generation: towards synergistic models of the JCT and inner wall endothelium. *Exp Eye Res*. 2009;88:656–670.
34. Ueda J, Wentz-Hunter K, Yue BY. Distribution of myocilin and extracellular matrix components in the juxtacanalicular tissue of human eyes. *Invest Ophthalmol Vis Sci*. 2002;43:1068–1076.
35. Yue BYJT. The extracellular matrix and its modulation in the trabecular meshwork. *Surv Ophthalmol*. 1996;40:379–390.
36. Rohen JW. Why is intraocular pressure elevated in chronic simple glaucoma? Anatomical considerations. *Ophthalmology*. 1983;90:758–765.
37. Johnson D, Gottanka J, Flugel C, Hoffmann F, Futa R, Lutjen-Drecoll E. Ultrastructural changes in the trabecular meshwork of human eyes treated with corticosteroids. *Arch Ophthalmol*. 1997;115:375–383.
38. Zhou L, Li Y, Yue BY. Glucocorticoid effects on extracellular matrix proteins and integrins in bovine trabecular meshwork cells in relation to glaucoma. *Int J Mol Med*. 1998;1:339–346.
39. Clark AF, Wilson K, de Kater AW, Allingham RR, McCartney MD. Dexamethasone-induced ocular hypertension in perfusion-culture human eyes. *Invest Ophthalmol Vis Sci*. 1995;36:478–489.
40. Johnson DH, Bradley JM, Acott TS. The effect of dexamethasone on glycosaminoglycans of human trabecular meshwork in perfusion organ culture. *Invest Ophthalmol Vis Sci*. 1990;31:2568–2571.
41. Tane N, Dhar S, Roy S, Pinheiro A, Ohira A, Roy S. Effect of excess synthesis of extracellular matrix components by trabecular meshwork cells: possible consequence on aqueous outflow. *Exp Eye Res*. 2007;84:832–842.
42. Zhang M, Maddala R, Rao PV. Novel molecular insights into RhoA GTPase-induced resistance to aqueous humor outflow through the trabecular meshwork. *Am J Physiol Cell Physiol*. 2008;295:C1057–C1070.
43. Yue BYJT. The extracellular matrix and its modulation in the trabecular meshwork. *Surv Ophthalmol*. 1996;40:379–390.
44. Aihara M, Lindsey JD, Weinreb RN. Ocular hypertension in mice with a targeted type I collagen mutation. *Invest Ophthalmol Vis Sci*. 2003;44:1581–1585.
45. Zanussi S, Doliana R, Segat D, Bonaldo P, Colombatti A. The human type VI collagen gene. mRNA and protein variants of the alpha 3 chain generated by alternative splicing of an additional 5-end exon. *J Biol Chem*. 1992;267:24082–24089.
46. Chu ML, Zhang RZ, Pan TC, et al. Mosaic structure of globular domains in the human type VI collagen alpha 3 chain: similarity to von Willebrand factor, fibronectin, actin, salivary proteins and aprotinin type protease inhibitors. *EMBO J*. 1990;9:385–393.
47. Pfaff M, Aumailley M, Specks U, Knolle J, Zerwes HG, Timpl R. Integrin and Arg-Gly-Asp dependence of cell adhesion to the native and unfolded triple helix of collagen type VI. *Exp Cell Res*. 1993;206:167–176.
48. Myint E, Brown DJ, Ljubimov AV, Kyaw M, Kenney MC. Cleavage of human corneal type VI collagen alpha 3 chain by matrix metalloproteinase-2. *Cornea*. 1996;15:490–496.
49. Lamandé SR, Sigalas E, Pan TC, et al. The role of the alpha3(VI) chain in collagen VI assembly. Expression of an alpha3(VI) chain lacking N-terminal modules N10-N7 restores collagen VI assembly, secretion, and matrix deposition in an alpha3(VI)-deficient cell line. *J Biol Chem*. 1998;273:7423–7430.
50. Martinek N, Shahab J, Sodek J, Ringuette M. Is SPARC an evolutionarily conserved collagen chaperone? *J Dent Res*. 2007;86:296–305.
51. Chlenski A, Guerrero LJ, Salwen HR, et al. Secreted protein acidic and rich in cysteine is a matrix scavenger chaperone. *PLoS One*. 2011;6:e23880.
52. Emerson RO, Sage EH, Ghoh JG, Clark JI. Chaperone-like activity revealed in the matricellular protein SPARC. *J Cell Biochem*. 2006;98:701–705.
53. Oh DJ, Martin JL, Williams AJ, et al. Analysis of expression of matrix metalloproteinases and tissue inhibitors of metalloproteinases in human ciliary body following latanoprost. *Invest Ophthalmol Vis Sci*. 2006;47:453–463.
54. Oh DJ, Martin JL, Williams AJ, Russell P, Birk DE, Rhee DJ. Effect of latanoprost on the expression of matrix metalloproteinases and their tissue inhibitors in human trabecular meshwork cells. *Invest Ophthalmol Vis Sci*. 2006;47:3887–3895.
55. McCurdy S, Baicu CF, Heymans S, Bradshaw AD. Cardiac extracellular matrix remodeling: fibrillar collagens and Secreted Protein Acidic and Rich in Cysteine (SPARC). *J Mol Cell Cardiol*. 2010;48:544–549.
56. Hohenester E, Sasaki T, Guidici C, Farndale RW, Bachinger HP. Structural basis of sequence-specific collagen recognition by SPARC. *Proc Natl Acad Sci U S A*. 2008;105:18273–18277.
57. Kandalam V, Basu R, Moore L, et al. Lack of tissue inhibitor of metalloproteinases 2 leads to exacerbated left ventricular dysfunction and adverse extracellular matrix remodeling in response to biomechanical stress. *Circulation*. 2011;124:2094–2105.
58. Chang W, Wei K, Jacobs SS, Upadhyay D, Weill D, Rosen GD. SPARC suppresses apoptosis of idiopathic pulmonary fibrosis fibroblasts through constitutive activation of beta-catenin. *J Biol Chem*. 2010;285:8196–8206.
59. Bhoopathi P, Chetty C, Gujrati M, Dinh DH, Rao JS, Lakka SS. The role of MMP-9 in the anti-angiogenic effect of secreted protein acidic and rich in cysteine. *Br J Cancer*. 2010;102:530–540.
60. Arnold SA, Rivera LB, Miller AF, et al. Lack of host SPARC enhances vascular function and tumor spread in an orthotopic murine model of pancreatic carcinomas. *Dis Model Mech*. 2010;3:57–72.
61. Atorrasagasti C, Aquino JB, Hofman L, et al. SPARC downstream attenuates the profibrogenic response of hepatic stellate cells induced by TGF-b1 and PDGF. *Am J Physiol Gastrointest Liver Physiol*. 2011;300:G739–G748.
62. Wei HY, Liu JL, Lv BJ, Xing L, Fu SY. SPARC modulates expression of extracellular matrix genes in human trabecular meshwork cells. *Acta Ophthalmol*. 2012;90:e138–e143.

Investigative Ophthalmology & Visual Science